The effect of energetic electron precipitation on middle mesospheric night-time ozone during and after a moderate geomagnetic storm

M. Daae,[1] P. Espy,[1] H. Nesse Tyssøy,[2] D. Newnham,[3] J. Stadsnes,[2] and F. Søraas[2]

[1]   Using a ground-based microwave radiometer at Troll Station, Antarctica (72°S, 2.5°E, $L = 4.76$), we have observed a decrease of 20–70% in the mesospheric ozone, coincident with increased nitric oxide, between 60 km and 75 km altitude associated with energetic electron precipitation ($E > 30$ keV) during a moderate geomagnetic storm (minimum Dst of -79 nT) in late July 2009. NOAA satellite data were used to identify the precipitating particles and to characterize their energy, spatial distribution and temporal variation over Antarctica during this isolated storm. Both the ozone decrease and nitric oxide increase initiate with the onset of the storm, and persist for several days after the precipitation ends, descending in the downward flow of the polar vortex. These combined data present a unique case study of the temporal and spatial morphology of chemical changes induced by electron precipitation during moderate geomagnetic storms, indicating that these commonplace events can cause significant effects on the middle mesospheric ozone distribution. **Citation:** Daae, M., P. Espy, H. Nesse Tyssøy, D. Newnham, J. Stadsnes, and F. Søraas (2012), The effect of energetic electron precipitation on middle mesospheric night-time ozone during and after a moderate geomagnetic storm, *Geophys. Res. Lett.*, *39*, L21811, doi:10.1029/2012GL053787.

1.   Introduction

[2]   Odd nitrogen ($NO_x = NO + NO_2$) catalytically destroys ozone (O_3) in the atmosphere, especially if it is created or transported below 40 km into the stratosphere where it is shielded from photo-dissociation and can survive for years. In the polar upper mesosphere during winter, the photochemical lifetime of NO_x is on the order of days due to the low elevation angles of the solar irradiance. This is long enough for NO_x to undergo both horizontal and vertical transport. Downward transport during the polar winter increases the lifetime of NO_x and enhances its impact on middle atmospheric O_3 [*Funke et al.*, 2005].

[3]   In the thermosphere, auroral particle precipitation, with electron energies typically less than 10 keV, is known to enhance NO_x production, particularly during the winter [e.g., *Sætre et al.*, 2004, and references therein]. A statistical study by *Hunt et al.* [2011] over solar cycle 24 shows a significant short-term correlation between the Ap-index and the infrared radiation from NO_x, indicating that even weak geomagnetic storms may enhance thermospheric NO_x densities. However, the rate of transport of this NO_x downward through the mesopause and into the middle atmosphere, where it can react with mesospheric and stratospheric O_3, is uncertain [*Smith et al.*, 2011].

[4]   During Solar Energetic Particle (SEP) events, direct production of NO_x in the middle atmosphere, caused mainly by large fluxes of high-energy protons with energies >100 MeV, has been observed and modeled [*Turunen et al.*, 2009]. This NO_x, as well as short-lived HO_x that is also produced, has been observed to create large decreases of stratospheric and mesospheric O_3 that persist throughout the winter [e.g., *Jackman et al.*, 2001]. However, since these events are relatively uncommon, occurring sporadically near solar maximum, their overall effect on middle atmospheric chemistry may be limited.

[5]   Long-term statistical studies show a strong correlation between Energetic Particle Precipitation (EPP) and NO_x levels in the polar middle atmosphere, along with an anti-correlation with O_3 abundance in the middle atmosphere [*Siskind et al.*, 2000], further indicating that geomagnetic storms weaker than SEPs may be important in middle atmospheric chemistry. *Newnham et al.* [2011] used ground-based radiometer observations to show that moderate geomagnetic storms, which occur frequently throughout the solar cycle, can produce large enhancements of mesospheric nitric oxide (NO).

[6]   In this work, using the same instrumentation employed by *Newnham et al.* [2011], we examine the case of a moderate geomagnetic storm that was relatively isolated in time. We show that not only did this storm produce a considerable enhancement of NO in the mesosphere, but also that this enhancement was accompanied by a substantial decrease of O_3 at the same altitudes. These ground-based data have been combined with satellite observations of the particle flux to characterize the energy deposition altitude, as well as the temporal and vertical evolution of the resulting NO and O_3 catalytic chemistry.

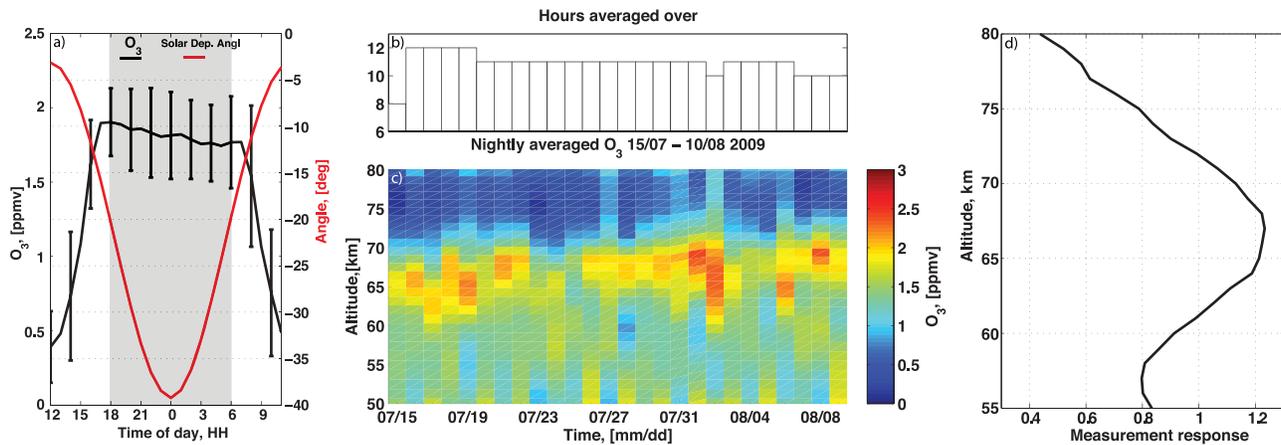[1]Department of Physics, Norwegian University of Science and Technology, Trondheim, Norway.
[2]Department of Physics, University of Bergen, Bergen, Norway.
[3]British Antarctic Survey, Cambridge, UK.

Corresponding author: P. Espy, Department of Physics, Norwegian University of Science and Technology, Høgskoleringen 5, N-7491 Trondheim, Norway. (patrick.espy@ntnu.no)

2.   Instruments and Method

[7]   A microwave radiometer was stationed at Troll, Antarctica, at 72°S and 2.5°E (62° Mlat, $L = 4.76$). The instrument operated at this location between early 2008 and early 2010, collecting spectral data from O_3, NO and CO [*Espy et al.*, 2006]. The radiometer measures thermal emissions from a rotational transition for NO centered at 250.796 GHz [*Newnham et al.*, 2011]. In addition, the

Figure 1. (a) The diurnal cycle of O_3 at 70 km altitude between 15 July and 10 August 2009 (black) and the solar elevation angle (red), grey area shows the time of day we pick O_3 profiles from. (b) The numbers of hourly O_3 profiles averaged each night. (c) Nightly averaged O_3 vmr between 15 July and 10 August 2009 in the mesosphere. (d) The averaged night-time measurement response for the O_3 inversion.

radiometer measures the O_3 line centred at 249.96 GHz using a 220 MHz bandwidth, 14.5 kHz resolution Chirp Transform Spectrometer, which, due to the brightness of this line and its spectral proximity to the NO line, can be observed simultaneously with NO. To increase the S/N we average over 200 spectra giving an hourly resolution for O_3 profiles. The O_3 spectra were inverted into volume mixing ratio (vmr) profiles using the Atmospheric Radiative Transfer Simulator (ARTS) as a forward model [*Buehler et al.*, 2005], and the optimal estimation technique of *Rodgers* [1976].

[8] Midnight *a priori* O_3 profiles at Troll were taken from a climatology generated with the Whole Atmosphere Community Climate Model (WACCM v3.5.48) [*Garcia et al.*, 2007], averaged over the years 2004–2007. In an effort to see if the daily *a priori* O_3 profiles used in the spectral inversion were affecting the inverted O_3 profiles, the spectra were also inverted using a constant *a priori* value above 50 km. The resulting O_3 values were not significantly different from those presented in this paper, and thus the results represent a real feature in the data and are not a product of the inversion method nor the *a priori* used.

[9] Figure 1d shows that the measurement response exceeds 80% from 57 km to 75 km, indicating that retrievals over this range are driven by observational data rather than *a priori* information. This altitude range includes the Middle Mesospheric Maximum (MMM) of O_3 which occurs at a nominal altitude of $\sim$72 km [*Marsh et al.*, 2001]. The MMM is known to have a strong diurnal cycle, where the O_3 vmr is greatly reduced in sunlight. The diurnal variation at 70 km, shown in Figure 1a, shows that an average covering the period when the sun is more than 20° below the horizon represents a mean nighttime O_3 value. The nightly average is taken from, for example, the evening of 21 July through the morning of 22 July (for solar elevation $< -20°$) and is referred to in the text and figures as the 22 July. The resulting nightly-averaged O_3 is shown in Figure 1c. The NO were processed using similar techniques [*Newnham et al.*, 2011] as for O_3 to give daily profiles between 60 km and 85 km.

The inversion is insensitive to NO above 85 km, and below 65 km NO converts to NO_2 in darkness.

[10] NOAA data [*Evans and Greer*, 2000] were used for characterizing the particle precipitation occurring over Troll during this event. Particle data were picked from an area covering $-72.0° \pm 1.0°$ latitude ($-60.5° \pm 0.5°$ Ilat) and 24°W to 67°E longitude. The proton spectra are corrected for degradation according to *Asikainen and Mursula* [2011] before they are converted into energy deposition profiles. In the first phase of the storm there was a significant flux of protons in the energy range 210–2700 keV which could contaminate the MEPED electron detector. Reliable spectra of Energetic Electron Precipitation (EEP) in the main phase therefore required a wider search. The METOP 02 data at 03:32 UT taken at -61.5 Ilat and -62.5 longitude were not contaminated by protons. We believe this profile represents the lower limit of electron energy deposition in the first phase of the storm as it was retrieved from the flanks of the main particle deposition region. Proton fluxes were low enough during the last part of the storm that the electron spectra could be corrected for contamination. The electron energy spectra are based on the three MEPED electron channels (>30 keV, >100 keV, >300 keV). We use the electron spectra to calculate the energy deposition as a function of altitude. In these calculations we use the cosine dependent IDH (Isotropic over the Downward Hemisphere) model of *Rees* [1989]. The proton energy spectra are based on five MEPED proton channels (30–80 keV, 80–250 keV, 250–800 keV, 800–2500 keV, 2500–6900 keV). The energy deposition height profile for protons is calculated based on range-energy of protons in air given by *Cook et al.* [1953] for $E < 300$ keV and by *Bethe and Ashkin* [1953] for $E > 300$ keV. We have assumed that the proton fluxes are isotropic over the downward hemisphere.

3. Results

[11] Figure 1c shows the O_3 mixing ratio as a function of altitude and time during the 26-day period between 15 July
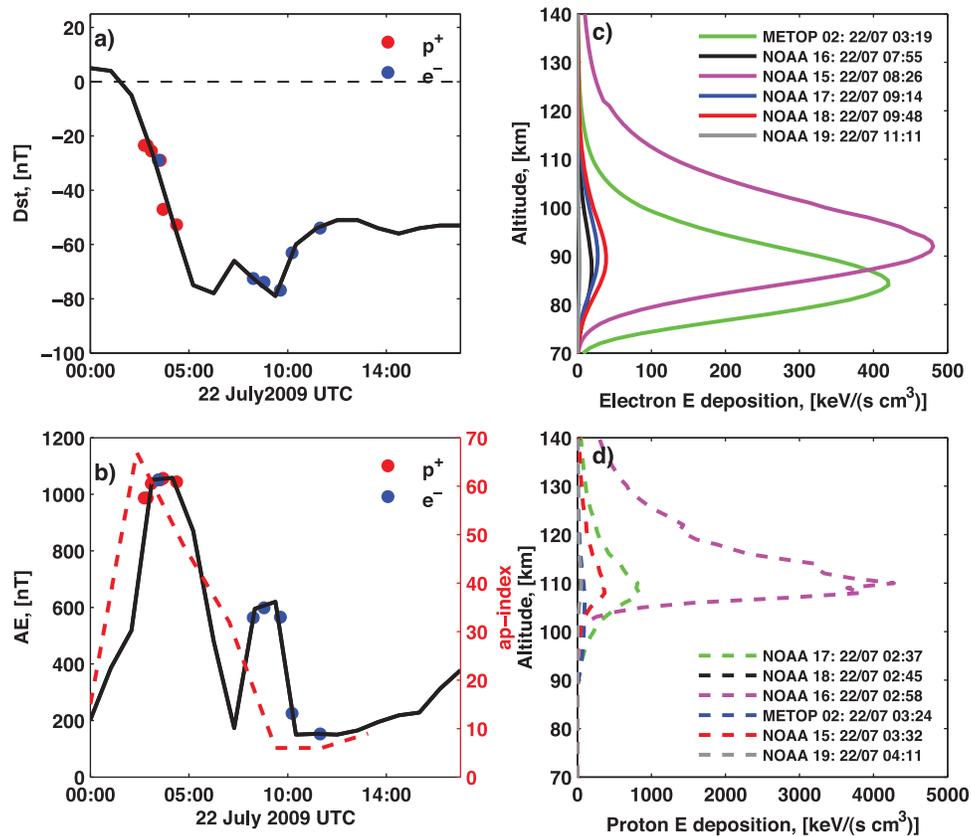
Figure 2. (a) *Dst*-index (black) with blue (red) dots indicating the times of the electron (proton) energy deposition altitude profiles. (b) Energy deposition altitude profiles from electrons in the magnetic local time morning side. (c) The *AE*- and *ap*- index. (d) Energy deposition altitude profiles of protons in the magnetic local time evening side.

and 10 August 2009. The maximum mesospheric O_3 vmr occurs between 65 km and 70 km. Since the measurement response is low above 75 km, the stronger secondary maximum near the mesopause ($\sim$95 km) is not observed. Nightly variations on the order of ± 0.5 ppmv due to wave-induced temperature fluctuations are seen to occur in the mesosphere [*Azeem et al.*, 2001]. However, a deeper and more persistent O_3 minimum appears on 22 July, corresponding to the onset of a moderate geomagnetic storm and lasts for about 1–2 weeks.

[12] The *Dst*-index (Figure 2a) shows that the storm reached -79 nT within the first 6 hours of 22 July, with the magnetosphere mostly recovering by the end of the day (seen in Figure 3a). The *AE*-index, although based on magnetometer data from the northern hemisphere, indicates (Figure 2b) that two bursts of precipitation occurred: one around 03:00 UT and a smaller burst around 09:00 UT. The energetic precipitation during both bursts in the *AE*-index occurs over a broad latitudinal range, extending 5 degrees equatorward and poleward of Troll (not shown).

[13] The electron- and proton- energy deposition profiles are displayed in Figures 2c and 2d respectively (explained in section 2), taken at the times marked by red/blue dots in Figures 2a and 2b. During the first burst of precipitation, electrons are seen to deposit their energy down to 70 km altitude coincident with the immediate reduction of O_3 observed in Figure 1c. While the electrons come into the

mesosphere, the protons are all stopped above 100 km, depositing their energy into the thermosphere. During the second burst of precipitation, electrons still deposit energy in the same region of the mesosphere where the reduction of O_3 is observed. At this time, the detectors do not register any significant proton fluxes. The high energy proton detectors $P6_{omni}$-$P7_{omni}$, covering energies > 16 MeV, from 0.8 MeV to 6.9 MeV, do not respond during this geomagnetic storm, indicating that there are no high-energy protons (or highly relativistic E > 800 keV electrons) present. Thus, it is unlikely that protons played a role in the O_3 decreases observed below 80 km.

[14] To further examine the O_3 reduction that coincided with the geomagnetic storm we have calculated O_3 anomalies; these are shown in Figure 3b. The anomalies were calculated by subtracting the O_3 profile averaged over the 7 days prior to the storm onset from each profile shown in Figure 1c, and are given in percentage relative to that 7-day average. The temporal behavior and spatial morphology of the O_3 loss are clearly seen. The O_3 shows a 17% reduction immediately following the storm onset at altitudes above 75 km, i.e., in the electron energy deposition region. The depletion above 70 km intensifies to 67% the following day, and gradually recovers over the next $\sim$2 days above this altitude. Figure 3b also shows that the reduced O_3 region extends and shifts to lower altitudes, with the centroid of the loss region reaching $\sim$60 km
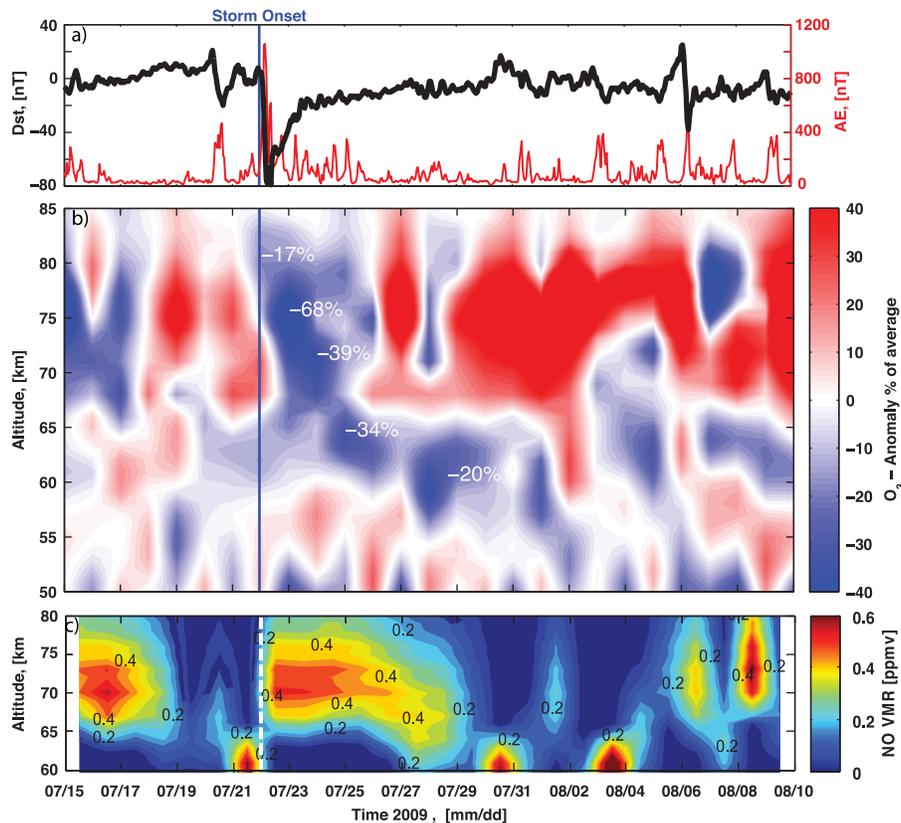
Figure 3. (a) Black (Red) line is the *Dst*-index (*AE*-index) from 15 July to 10 August 2009, blue vertical bar shows storm onset. (b) Mesospheric O_3 anomalies relative to a 7-day average prior to storm onset. Values are given in percentage of the 7-day average. Numbers on the plot highlight O_3 depletion at different altitudes and times. (c) Daily NO vmr profiles.

in ~5 days and continuing down to 55 km ~12 days after the storm onset, after which the feature is lost.

[15] The observed daily NO profiles during the time investigated are shown in Figure 3c. The NO abundance increased to 0.5 ppmv the day following the storm. This increase occurred the same day as O_3 depletion becomes evident in the MMM O_3. The NO increase follows the same pattern as the O_3 depletion, persisting between 65 km and 80 km for the first four days after the storm onset before propagating downward, reaching 60 km ~5 days after storm onset.

4. Conclusions and Discussion

[16] During 22 July 2009 a moderate geomagnetic storm occurred reaching its maximum at 10:00 UT as characterized by the *Dst*-index (−79 nT). Two precipitation bursts occurred during the storm, with considerable precipitation by electrons in the 30 keV to 300 keV range that deposited their energy directly in the upper mesosphere above 70 km. As the main precipitation came into the mesosphere close to sunrise, only a minor decrease is seen in the O_3 during the night of the storm. However, on the following night, 22/23 July, the nightly-averaged O_3 was depleted by almost 70% above 70 km, accompanied by a strong enhancement of NO at the same altitudes. This region of decreased O_3 persisted at altitudes higher than 70 km for about 4 days. The centroid of the O_3 depletion is observed to move downwards to 55 km within 12 days after storm onset. Thus, the depletion moved downward at a speed of ~1–3 cm/s in agreement with previous modeling results of the vertical wind at these altitudes

[e.g., *Garcia and Solomon*, 1985; *Sheese et al.*, 2011]. NO was observed to move downwards to ~60 km, tracking the behavior of the O_3 depletion at the same altitudes. Below 60 km, the NO vmr falls below the instrument sensitivity due to the shift of the NO_x balance from NO to NO_2. Thus, while NO is not retrieved below 60 km, it is likely that NO_x was still actively keeping the O_3 levels depressed.

[17] Given the appearance of the NO enhancement and O_3 reduction concurrent with the precipitation, coupled with the downward propagation times above 80 km, it appears that NO produced in the mesosphere, rather than downward transported thermospheric NO, was the dominant cause of O_3 loss during this storm. There may also have been a contribution to O_3 loss from HO_x produced during the precipitation [*Verronen et al.*, 2011]. However, HO_x is short lived and rapidly photodissociated. In addition, the middle mesospheric maximum, where O_3 loss is observed, owes its existence to photo-chemical conditions that result in any photo-dissociated HO_x rapidly returning to stable chemical reservoirs [*Marsh et al.*, 2001]. Thus, the timing of the precipitation just before and during daylight, as well as the observed persistence of the O_3 loss (beyond the particle precipitation) and its coincidence with enhanced NO, indicates that during this event the O_3 loss was predominantly due to NO produced in the upper mesosphere by energetic electron precipitation.

5. Summary

[18] Our study shows for the first time how a 12-hour long moderate geomagnetic storm can cause chemical changes

to the middle mesosphere. The night-time mesospheric O_3 column was depleted by 20–70% relative to the average values prior to the storm. A coincident NO increase was measured with the same instrument and, given this coincidence and duration of the O_3 depletion, it is likely that NO was the active destructor in the loss of O_3. The total impact of the storm reached down to 55 km altitude within 12 days giving a vertical decent velocity of 1–3 cm/s.

[19] Storms of this size occur frequently throughout a typical 11-year solar cycle. Given the large effect on atmospheric chemistry observed here, this implies that particle precipitation can have a significant day-to-day impact on middle atmospheric chemistry. This has been indicated several times by long-term statistical studies [e.g., *Callis et al.*, 2001]. Although solar activity was unusually low during 2009, under more normal conditions, storms of similar size may recur every 1–2 weeks, possibly causing a persistent suppression of middle mesospheric O_3.

[21] The Editor thanks Edward Llewellyn for his assistance in evaluating this paper.

References

Asikainen, T., and K. Mursula (2011), Energetic electron flux behavior at low L-shells and its relation to the South Atlantic anomaly, *J. Atmos. Sol. Terr. Phys.*, *70*, 532–538.

Azeem, S. M. I., S. E. Palo, D. L. Wu, and L. Froidevaux (2001), Observations of the 2-day wave in UARS MLS temperature and ozone measurements, *Geophys. Res. Lett.*, *28*, 3147–3150.

Bethe, H., and J. Ashkin (1953), *Passage of Radiations Through Matter*, *Part II of Experimental Nuclear Physics*, vol. 1, John Wiley, New York.

Buehler, S., P. Eriksson, T. Kuhn, A. von Engeln, and C. Verdes (2005), ARTS the Atmospheric Radiative Transfer Simulator, *J. Quant. Spectrosc. Radiat. Transfer*, *91*, 65–93.

Callis, L. B., M. Natarajan, and J. D. Lambeth (2001), Solar-atmospheric coupling by electrons (SOLACE): 3. Comparisons of simulations and observations, 1979–1997, issues and implications, *J. Geophys. Res.*, *106*, 7523–7539.

Cook, C. J., E. Jones, and T. Jorgensen (1953), Range-energy relations of 10 to 250 keV protons and helium ions in various gases, *Phys. Rev.*, *91*, 1417–1422.

Espy, P., P. Hartogh, and K. Holmén (2006), A microwave radiometer for the remote sensing of nitric oxide and ozone in the middle atmosphere, in *Remote Sensing of Clouds and the Atmosphere XI*, *Proc. SPIE*, *6362*, 1–9.

Evans, D. S., and M. S. Greer (2000), Polar Orbiting Environmental Satellite Space Environment Monitor 2: Instrument description and archive data documentation, *NOAA Tech. Memo. OAR SEC-93*, NOAA, Boulder, Colo.

Funke, B., M. López-Puertas, S. Gil-López, T. von Clarmann, G. P. Stiller, H. Fischer, and S. Kellmann (2005), Downward transport of upper atmospheric NOx into the polar stratosphere and lower mesosphere during the Antarctic 2003 and Arctic 2002/2003 winters, *J. Geophys. Res.*, *110*, D24308, doi:10.1029/2005JD006463.

Garcia, R. R., and S. Solomon (1985), The effect of breaking gravity waves on the dynamics and chemical composition of the mesosphere and lower thermosphere, *J. Geophys. Res.*, *90*, 3850–3868.

Garcia, R. R., D. R. Marsh, D. E. Kinnison, B. A. Boville, and F. Sassi (2007), Simulation of secular trends in the middle atmosphere, 1950–2003, *J. Geophys. Res.*, *112*, D09301, doi:10.1029/2006JD007485.

Hunt, L. A., M. G. Mlynczak, B. T. Marshall, C. J. Mertens, J. C. Mast, R. E. Thompson, L. L. Gordley, and J. M. Russell III (2011), Infrared radiation in the thermosphere at the onset of solar cycle 24, *Geophys. Res. Lett.*, *38*, L15802, doi:10.1029/2011GL048061.

Jackman, C. H., R. D. McPeters, G. J. Labow, E. L. Fleming, C. J. Praderas, and J. M. Russell (2001), Northern Hemisphere atmospheric effects due to the July 2000 Solar Proton Event, *Geophys. Res. Lett.*, *28*(15), 2883–2886.

Marsh, D., A. Smith, G. Brasseur, M. Kaufmann, and K. Grossmann (2001), The existence of a tertiary ozone maximum in the high-latitude middle mesosphere, *Geophys. Res. Lett.*, *28*, 4531–4534.

Newnham, D. A., P. J. Espy, M. A. Clilverd, C. J. Rodger, A. Seppälä, D. J. Maxfield, P. Hartogh, K. Holmén, and R. B. Horne (2011), Direct observations of nitric oxide produced by energetic electron precipitation into the Antarctic middle atmosphere, *Geophys. Res. Lett.*, *38*, L20104, doi:10.1029/2011GL048666.

Rees, M. H. (1989), *Physics and Chemistry of the Upper Atmosphere*, Cambridge Univ. Press, Cambridge, U. K.

Rodgers, C. (1976), Retrieval of atmospheric temperature and composition from remote measurements of thermal radiation, *Rev. Geophys.*, *14*, 609–624.

Sætre, C., J. Stadsnes, H. Nesse, A. Aksnes, S. M. Petrinec, C. A. Barth, D. N. Baker, R. R. Vondrak, and N. Østgaard (2004), Energetic electron precipitation and the NO abundance in the upper atmosphere: A direct comparison during a geomagnetic storm, *J. Geophys. Res.*, *109*, A09302, doi:10.1029/2004JA010485.

Sheese, P. E., R. L. Gattinger, E. J. Llewellyn, C. D. Boone, and K. Strong (2011), Nighttime nitric oxide densities in the Southern Hemisphere mesosphere–lower thermosphere, *Geophys. Res. Lett.*, *38*, L15812, doi:10.1029/2011GL048054.

Siskind, D. E., G. E. Nedoluha, C. E. Randall, M. Fromm, and J. M. Russell III (2000), An assessment of Southern Hemisphere stratospheric NO_x enhancements due to transport from the upper atmosphere, *Geophys. Res. Lett.*, *27*, 329–332.

Smith, A. K., R. R. Garcia, D. R. Marsh, and J. H. Richter (2011), WACCM simulations of the mean circulation and trace species transport in the winter mesosphere, *J. Geophys. Res.*, *116*, D20115, doi:10.1029/2011JD016083.

Turunen, E., P. T. Verronen, A. Seppälä, C. J. Rodger, M. A. Clilverd, J. Tamminen, C.-F. Enell, and T. Ulich (2009), Impact of different energies of precipitating particles on NO_x generation in the middle and upper atmosphere during geomagnetic storms, *J. Atmos. Sol. Terr. Phys.*, *71*, 1176–1189.

Verronen, P. T., C. J. Rodger, M. A. Clilverd, and S. Wang (2011), First evidence of mesospheric hydroxyl response to electron precipitation from the radiation belts, *J. Geophys. Res.*, *116*, D07307, doi:10.1029/2010JD014965.